Nuclear Data for Science and Technology (1988 MITO), 999-1002, Copyright © 1988 JAERI.

ACTIVATION OF STRUCTURAL MATERIALS DUE TO RECOIL PROTONS IN LIGHT WATER REACTOR

Masato Takahashi and Shungo Iijima

NAIG Nuclear Research Laboratory
4-1, Ukishima-cho, Kawasaki-ku, Kawasaki, 210 Japan

Abstract The long-lived radioactivities of structural materials induced by recoil protonss in BWR were estimated for land disposal of low level waste after reactor decommisioning. Products of interest are Mn-53, Nb-91, Nb-94, Tc-97, Sb-125, Lu-173 and Lu-174. Method of calculation of the proton spectrum in materials was presented. Program PEGASUS-P was developed by modifying PEGASUS, a preequilibrium and multistep evaporation theory code, to calculate proton reaction cross sections. The proton-induced activity is shown as not exceeeding 1/1000 of that of a typical neutron induced activity of Ni-63 for cooling up to 1000 y after irradiation of 40 y in BWR.

(BWR, recoil proton, induced activity, structural material, proton cross section)

Introduction

It is important to estimate accurately the radio-activities of the low level waste for land disposal after the decommissioning of reactor. The activities have been evaluated hitherto based mostly on the neutron induced reactions. However, in the core of Light Water Reactor(LWR), high energy recoil protons are produced via scattering of fission neutrons with water. These protons impinge on the fuel cladding or other structural materials inducing radioactivities by proton reactions. (We note here an early work by Tagami et al./1/ on the production of N-13 in coolant water by reaction of recoil protons with O-16 atoms.) The long-lived isotopes of interest are Mn-53, Nb-91, Nb-94, Tc-97, Sb-125, Lu-173 and Lu-174. These are produced by proton reactions with stainless steel, inconel or zircaloy. The resultant activities were calculated for irradiation of 40 years in a typical BWR and subsequent cooling. These were compared with that of Ni-63 (half-life of 100y) which is a typical long-lived isotope produced by the neutron reaction with the structural materials.

Method of Calculation

Figure 1 shows a BWR lattice configuration. Fission neutrons born in fuel, escaping from fuel and colliding with water, give rise to the high energy recoil protons, some of which impinge on the structural materials and cause nuclear reactions. Table 1 lists the nuclides produced by proton reactions having half-lives longer than 1 y and reaction thresold energies less than 10 MeV.

Ignoring the neutron absorption and moderation by the collision with oxygen atoms in water, the recoil proton source spectrum is given by,

$$Q(E_p) = \nu \Sigma_f \phi_{th} f \int_{E_p}^{\infty} dE/E \left[\chi(E)+(1/E)\int_{E}^{\infty}\chi(E')dE'\right] \quad (1)$$

Here Φ_{th} is the thermal neutron flux in fuel, χ is the normalized thermal fission neutron spectrum, and f the fraction of neutrons that escape from fuel and make collisions with water. The factor f may be taken as the order of magnitude of 0.5.

Protons born in water attenuate mostly within it, but those born near material surface bombard the materials. Assuming that the protons are born uniformly and isotropically in water, the average proton flux spectrum in structural material is calculated as,

$$\phi_M(E) = (S/4V)/S_M(E)\int_{E}^{\infty} dE_p Q(E_p)\,[R_w(E_p)-R_w(E)] \quad (2)$$

Hence the reaction rate/atom/s is

$$R = \int_{o}^{\infty}\sigma(E)\phi_M(E)dE \quad (3)$$

Here, S_m is the proton stoping powers of the material and R_w the proton range in water. S and V are the surface area and volume of the material.

Eq.(3) is also expressed in terms of the thick target proton yield by

$$R = (S/4V)\int_{0}^{\infty} dE_o\, Q(E_o)\int_{0}^{E_p} dE\, Y(E)/S_w(E) \quad (4)$$

$$Y(E_p) = \int_{o}^{E_p}\sigma(E)/S_M(E)$$

Since Φ_M is proportional to thermal neutron flux, the reaction rate is given in terms of the effective thermal cross section defined by,

$$\sigma_{eff} = R/\phi_{th} \quad (5)$$

This can be compared directly with the effective thermal neutron cross section for production of Ni-63 by neutron capture rection with Ni-62 :

$$\sigma^* = \sqrt{\pi T_0/4T_n}\ \sigma_{2200} + rI$$

Here, T = 293K, T_n the neutron temperature, r the epithermal index, and I the resonance integral. Taking T_n = 1123K, r=0.165, σ_{2200} =14.5 b and I=6.6 b, we obtain σ^* = 7.7 b.
Compositions of structural materials were taken from ref.2. The U-235 thermal neutron fission spectrum was adopted from the NBS recommendation. The proton stopping powers in water, SUS and Zircaloy-2 were constructed from the elemental stopping power data of Ziegler/3/. The void volume fraction of 40 % was assumed for water. For other parameters, $\nu\Sigma_f$ was taken as 0.075 cm^{-1} and S/4V as 1.0 (equivalently the fuel radius or channel box thickness of 0.5 cm). Themal neutron flux value was taken as 4×10^{13} $n/cm^2/s$. These values are typical of the operating BWR's.

The calculated proton source spectrum Q(Ep), and the average spectra in water and structural materials are depicted in Fig. 2. It is seen that the protons of energy grerater than about 10 MeV do not contribute significantly to reactions. The integrated fluxes relative to thermal neutron flux are 2.15×10^{-4}, 5.7×10^{-7}, and 3.9×10^{-7} in water, Zircaloy-2 and SUS, respectively, showing a considerable reduction of proton reactions compared with neutron reactions.

Proton Reaction Cross Sections

Proton reactions with thresholds less than 10 MeV are of significance. The reaction cross sections were calculated with PEGASUS-P, a version of PEGASUS /4/, a preequilibrium and mutistep evporation theory code. Preequilibrium effect was ignored since it is not effective for proton energy below 10 MeV. As to the inverse cross sections, the formula of Pearlstein/5/ was adopted for neutrons. For charged particles the optical model calculation was used with potentials of Perey/6/, Huizenga and Igo/7/ and Lohr and Haeberli/8/, respectively, for protons, alphas and deuterons.

The level density parameters of Gilbert-Cameron type were determined from the neutron resonance and the lowlying level scheme data. Systematics was used when necessary.

Figure 3 shows the the calculated and measured (p,n) cross sections for Cu-63 and Cu-65. Level density parameters have been adjusted to some extent. Uncertainties of the factor of 2-to-3 have to be allowed in the calculated cross sections when experimental data are not available.

Resutls and Discussions

In upper part of Figs. 4(a) and 4(b) are shown respectively the thick target yields for production of Nb-91 and Lu-173 in zircaloy-2. Lower part of figures show the response function of the production of these nuclides and the main contributing reaction cross sections (dotted line).

The effective activation cross sections and reaction rates are given in Table 2. The induced activities per gram of material are given in the rightmost column for irradiation of 40 years. At the bottom of Table is given the neutron-induced Ni-63 activity for the sake of comaparison.

As seen from Table 2, the Nb-91 activity produced in Zircaloy-2 is dominant among proton induce activities. It is still by a factor of 1/10,000 smaller than that of Ni-63.

Figure 5 shows the activity per gram of parent materials as a function of cooling time after irradiation of 40 years. For cooling time up to 1000 years, the proton induced activities are less than 1/1000 of the Ni-63 activity. It is concluded that the activities due to recoil protons may be safely ignored by the land disposal of low level waste. The conclusion is believed to hold also for the case of PWR.

Acknowledgement

We owe to T.Sugi and T.Nakagawa at JAERI for use of the charged particle inverse cross section file. H. Mizuta at NAIG provided us with the nuetronics results on operating BWR's. We appreciate the discussions with T. Murata and Y. Yuasa at NAIG. Pioneering work by T. Tagami, late M. Yamamoto and T. Osawa at Hitachi was instructive to the present study.
We regret deeply the loss of M.Yamamoto.

REFERENCES

1. Tagami,T., Yamamoto,M., Osawa,T. : J. Atom. Energy Soc. Japan 17 12(1964) (in Japanese)
2. ORNL-TM-9591 (1986)
3. H.H. Anderson and J.F. Ziegler : Hydrogen, Stopping Powers and Ranges in All Elements, Vol.3 of the Stopping and Ranges of Ions in Matter, organized by J.F.Ziegler, Pergamon Press (1977)
4. S. Iijima, T. Sugi, T. Nakagawa and T. Nishigori: Program PEGASUS, JAERI-M 87-025 (1987) 3372.
5. S. Pearlstein : J.Nucl. Energy 27 88 (1973)
6. F.G. Perey : Phys. Rev. 181 745 (1963)
7. J.R. Huizenga and G.Igo : Nucl.Phys. 29 462 (1962)
8. J.M.Lohr and W.Haeberli : Nucl.Phys. A232 381 (1974)

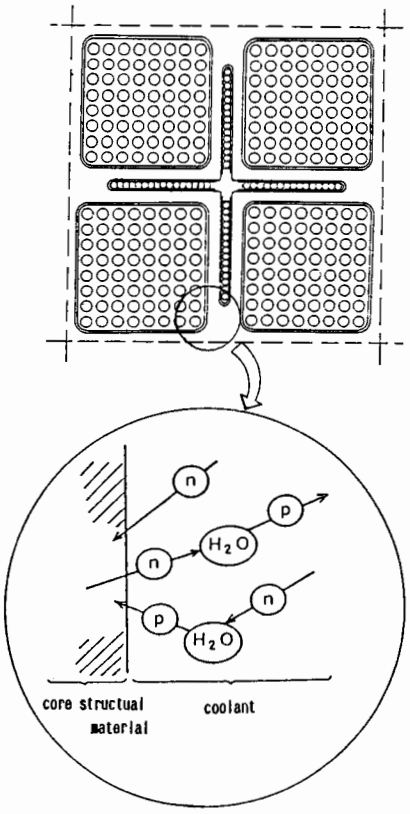

Fig.1 Production of recoil protons in BWR lattice.

Table 1 List of radioactive nuclides of interest produced by proton reactions ($T_{1/2}$ > 1y).

product nuclide	production mode			
Al-26g	^{27}Al (p, pn)	^{29}Si (p, α)	^{30}Si (p, αn)	^{27}Al (p, d)
Cl-36	^{36}S (p, n)			
Mn-53	^{52}Cr (p, γ)	^{53}Cr (p, n)	^{56}Fe (p, α)	^{57}Fe (p, αn)
Fe-55	^{55}Mn (p, n)	^{56}Fe (p, pn)	^{59}Co (p, αn)	^{56}Fe (p, d)
Co-60	^{64}Ni (p, αn)			
Ni-59	^{59}Co (p, n)	^{60}Ni (p, pn)	^{63}Cu (p, αn)	^{60}Ni (p, d)
Ni-63	^{64}Ni (p, pn)	^{64}Ni (p, d)		
Zr-93	^{94}Zr (p, pn)	^{94}Zr (p, d)		
Nb-91	^{90}Zr (p, γ)	^{91}Zr (p, n)	^{92}Zr (p, 2n)	^{93}Nb (p, dn)
	^{94}Mo (p, α)	^{95}Mo (p, αn)		
Nb-92	^{91}Zr (p, γ)	^{92}Zr (p, n)	^{93}Nb (p, d)	^{94}Mo (p, dp)
	^{95}Mo (p, α)	^{96}Mo (p, αn)		
Nb-93	^{92}Zr (p, γ)	^{94}Zr (p, 2n)	^{95}Mo (p, dp)	^{96}Mo (p, α)
	^{97}Mo (p, αn)			
Nb-94	^{94}Zr (p, n)	^{96}Mo (p, dp)	^{97}Mo (p, α)	^{98}Mo (p, αn)
Mo-93	^{93}Nb (p, n)	^{94}Mo (p, pn)	^{95}Mo (p, pn)	^{94}Mo (p, d)
	^{95}Mo (p, d)			
Tc-97	^{96}Mo (p, γ)	^{97}Mo (p, n)	^{98}Mo (p, 2n)	
Tc-98	^{97}Mo (p, γ)	^{98}Mo (p, n)		
Tc-99	^{100}Mo (p, 2n)			
Ag-108m	^{110}Cd (p, dp)	^{111}Cd (p, α)	^{112}Cd (p, αn)	
Cd-109	^{110}Cd (p, pn)	^{111}Cd (p, dn)	^{110}Cd (p, d)	
Cd-113m	^{114}Cd (p, pn)	^{114}Cd (p, d)		
Sn-121m	^{122}Sn (p, pn)	^{122}Sn (p, d)		
Sb-125	^{124}Sn (p, γ)			
Hf-172	^{174}Hf (p, dn)			
Hf-178m	^{179}Hf (p, pn)	^{180}Hf (p, dn)	^{179}Hf (p, d)	
Lu-173	^{176}Hf (p, α)	^{177}Hf (p, αn)		
Lu-174g	^{176}Hf (p, dp)	^{177}Hf (p, α)	^{178}Hf (p, αn)	
Ta-179	^{178}Hf (p, γ)	^{179}Hf (p, n)	^{180}Hf (p, 2n)	^{182}W (p, α)
	^{183}W (p, αn)			
Re-186m	^{186}W (p, n)			

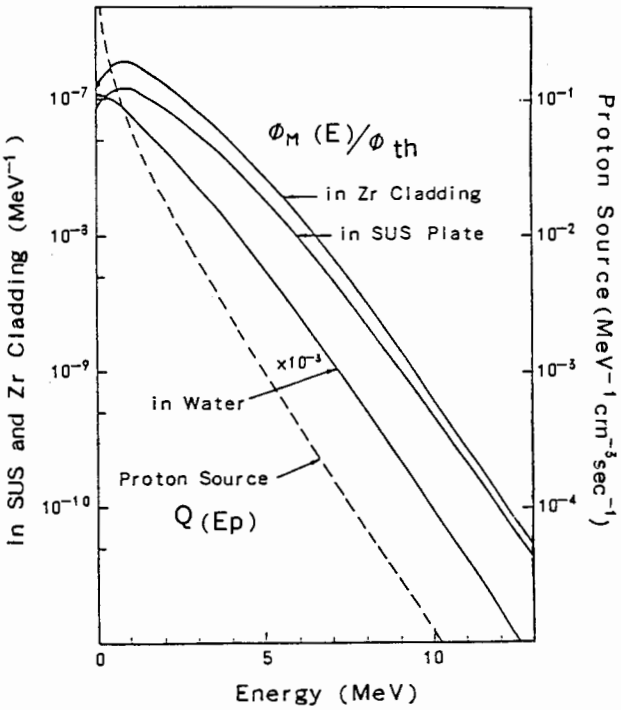

Fig.2 Proton source spectrum in water and the average proton spectra in water and structual materials.

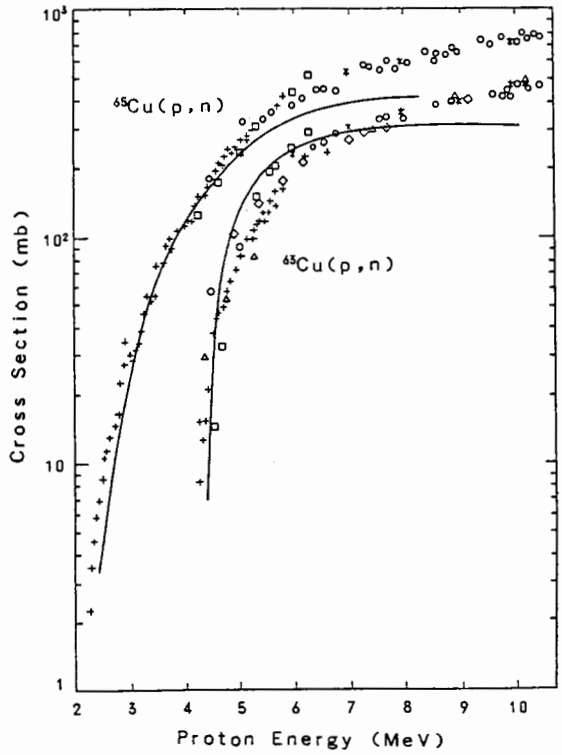

Fig.3 ^{63}Cu(p,n) and ^{65}Cu(p,n) cross sections. Comparison of caluculation with experiment. Solid curves are the result of calculated with PEGASUS code, and the marks of +, *, ○, △, □ and ◇ are experimental data.

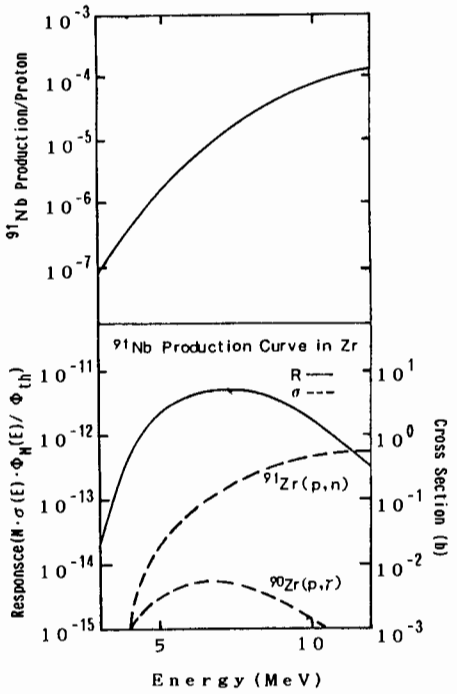

Fig.4 (a) Total response function and dominant contributing cross sections for production of ^{91}Nb in Zircaloy-2. Thick target yield is also depicted.

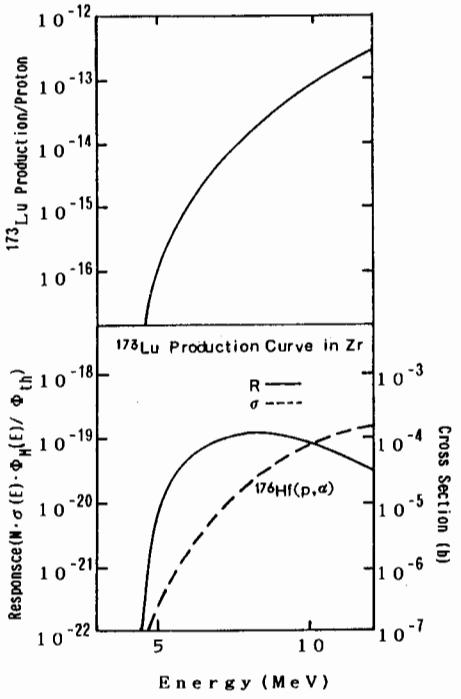

Fig.4 (b) Total response function and dominant contributing cross sections for production of ^{173}Lu in Zircaloy-2. Thick target yield is also depicted.

Table 2 The effective cross sections and induced radioactivities in materials after irradiation of 40 year in BWR.

STRUCTURAL MATERIAL	NUCLIDE	PRODUCTION MODE	EFFECFIVE CROSS SECTION (barn)	REACTION RATE (REACTIONS/g·sec)	ACTIVITY (μci/g)
ZIRCALOY − 2	Nb−91 (6.8×10^{2}y)	^{90}Zr (p,r)	4.9×10^{-10}	9.1×10^{2}	6.1×10^{-5}
		^{91}Zr (p,n)	1.2×10^{-8}	4.8×10^{5}	
		^{94}Mo (p,α)	1.5×10^{-10}	—	
		^{92}Mo (p,2p)	1.1×10^{-16}	—	
	Nb−94 (2.0×10^{4}y)	^{94}Zr (p,n)	1.3×10^{-8}	8.1×10^{5}	3.1×10^{-4}
	Sb−125 (3.2 y)	^{124}Sn (p,r)	4.9×10^{-11}	1.3×10^{-1}	3.4×10^{-6}
INCONEL 718	Mn−53 (3.7×10^{6}y)	^{52}Cr (p,r)	6.8×10^{-10}	3.5×10^{2}	2.0×10^{-7}
		^{53}Cr (p,r)	9.8×10^{-9}	5.7×10^{2}	
		^{54}Cr (p,r)	7.2×10^{-12}	1.0×10^{-1}	
		^{56}Fe (p,α)	7.4×10^{-11}	3.7×10^{1}	
		^{54}Fe (p,2p)	7.8×10^{-16}	2.4×10^{-5}	
ZIRCALOY − 2	Ni−63 (1.0×10^{2}y)	^{62}Ni(n,r)	8.6	4.4×10^{8}	2.9×10^{5}

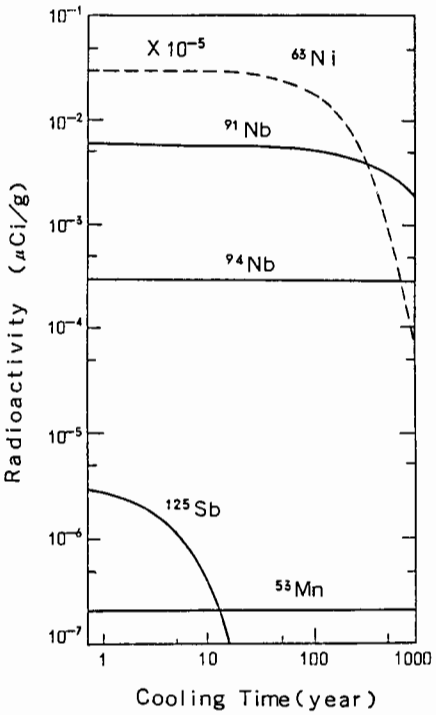

Fig.5 Proton induced radioactivities of main long-lived isotopes as a function of cooling time after irradiation of 40 years in BWR in comparison with neutron-induced ^{63}Ni activity.